Available online at www.sciencedirect.com
ScienceDirect
Journal of Power Sources 181 (2008) 31–37
JOURNAL OF POWER SOURCES
www.elsevier.com/locate/jpowsour

Evaluation of porous 430L stainless steel for SOFC operation at intermediate temperatures

Sebastian Molin [a], Boguslaw Kusz [b], Maria Gazda [b], Piotr Jasinski [a,*]

[a] *Faculty of Electronics, Telecommunication and Informatics, Gdansk University of Technology, ul. Narutowicza 11/12, 80-952 Gdansk, Poland*
[b] *Faculty of Applied Physics and Mathematics, Gdansk University of Technology, ul. Narutowicza 11/12, 80-952 Gdansk, Poland*

Received 2 October 2007; accepted 3 October 2007
Available online 9 October 2007

Abstract

In this paper a 430L porous stainless steel is evaluated for possible SOFC applications. Recently, there are extensive studies related to dense stainless steels for fuel cell purposes, but only very few publications deal with porous stainless steel. In this report porous substrates, which are prepared by die-pressing and sintering in hydrogen of commercially available 430L stainless steel powders, are investigated. Prepared samples are characterized by scanning electron microscopy, X-ray diffractometry and cyclic thermogravimetry in air and humidified hydrogen at 400 °C and 800 °C. The electrical properties of steel and oxide scale measured in air are investigated as well. The results show that at high temperatures porous steel in comparison to dense steel behaves differently. It was found that porous 430L has reduced oxidation resistance both in air and in humidified hydrogen. This is connected to its high surface area and grain boundaries, which after sintering are prone to oxidation. Formed oxide scale is mainly composed of iron oxide after the oxidation in air and chromium oxide after the oxidation in humidified hydrogen. In case of dense substrates only chromium oxide scale usually occurs. Iron oxide is also a cause of relatively high area-specific resistance, which reaches the literature limit of 100 mΩ cm^2 when oxidizing in air only after about 70 h at 800 °C.

Keywords: 430L stainless steel; Porous stainless steel; SOFC metal support

1. Introduction

Solid oxide fuel cells (SOFC) are very promising energy sources. They are offering the highest available energy efficiencies due to conversion of chemical energy of the electrochemical oxidation reaction of fuel directly into electrical energy. Possible applications include auxiliary power units for homes, hospitals, trucks, etc. Although the main barrier for their widespread commercialization is high cost. This problem can be overcome by use of less expensive materials, e.g. stainless steel as an interconnector. Recently, advanced electrolyte deposition technologies [1] allowed fabrication of thin electrolyte layers (below 10 μm), which allows to lower temperature of operation without increasing electrolyte resistance above acceptable level. Temperatures in the range of 500–800 °C provide an opportunity to use stainless steels as an interconnector or support. There are currently only a few steels that are considered for SOFC application. Main problem with use of steel at elevated temperatures is its high-temperature corrosion and thermal expansion coefficient (TEC) mismatch between steel and ceramics. This first problem can be partially solved by using chromia forming alloys [2] that form passivation layer of Cr_2O_3, which protects steel interior from further degradation and reveal good electrical conductivity. TEC problem is minimized once ferritic stainless steels are used, which are well-matched with TEC, to the most popular ceramics—yttria stabilized zirconia ($TEC_{YSZ} \sim 10$ ppm K^{-1} and $TEC_{430L} \sim 11.4$ ppm K^{-1} [3]).

Ferritic steels, which are typically studied for SOFC applications, include popular 430 series and specially developed alloys, e.g. Crofer22APU (ThyssenKrupp VDM) E-Brite (Allegheny Ludlum) and ZMG232 (Hitachi Metals Ltd.). In addition some nickel-based alloys (austenitic crystal structure) are also taken into account, e.g. Haynes 230 and Haynes 242 (Haynes International). Table 1 presents their typical composition. The high percent of chromium ensures formation of protective chromia scale, while other atom additives are chosen to form scales

* Corresponding author. Tel.: +48 58 3471323; fax: +48 58 3471757.
E-mail address: pijas@eti.pg.gda.pl (P. Jasinski).

0378-7753/$ – see front matter © 2007 Elsevier B.V. All rights reserved.
doi:10.1016/j.jpowsour.2007.10.009

Table 1
Main alloying elements in steels used as SOFC interconnects [wt%]

Steel	Fe	Cr	Mn	C	Mo	Ni	Other:	Reference
430	>77.0	16.0–18.0	<1.0	<0.12	<0.5	–	Si < 1.0	[25]
Crofer 22 APU	>72.0	20.0–24.0	<0.8	<0.03	–	–	Cu < 0.5 Al < 0.5	[26]
E-brite	>70.0	26.0–27.5	<0.4	<0.01	<1.5	<0.5	Ni + Cu < 0.5 Nb < 0.2	[27]
Haynes 230	<3.0	22.0	0.5	0.1	2.0	<57.0	W—14.0 Co—5.0	[28]

on the surface of chromia and in this way restrict chromium vaporization [4,5]. The volatile chromia, which deposits on the cathode/electrolyte interface, degrades the fuel cell performance by blocking oxygen reduction sites [6]. The ferritic steels have been widely characterized as dense substrates [7–9]. In this case the steel is used as a current collector and as a physical barrier preventing fuel and oxidant mixing. In such cells one of the ceramic layers must act as a supporting structure and anode-supported configuration is often used [10,11].

The 430 dense steel has been thoroughly evaluated in SOFC conditions. Brylewski et al. [12,13] studied the oxidation kinetics in H_2–H_2O gas mixtures and in air in temperature range of 750–900 °C for duration of up to 300 h. It was shown that oxide scale is mainly composed of chromium oxide and grows according to parabolic Wagner relation. It was claimed that rates of oxidation are independent of oxygen partial pressures. Moreover, the steel coated with (La,Sr)CoO_3 exhibited average area-specific resistances of 20 mΩ cm^2 and 45 mΩ cm^2 in air and humidified hydrogen, respectively. Deng et al. [14] have successfully electroplated 430 stainless steel by cobalt that greatly decreased its area-specific resistance. In this case after 1900 h of oxidation in air at 800 °C the contact resistance of 26 mΩ cm^2 was obtained. Presented works show that the 430 dense stainless steel can be regarded as prospective for high-temperature SOFC interconnector.

Recently porous steel was successfully used as supporting structure in planar type SOFC [15–19]. Villarreal et al. [16] built cells on porous 70Fe30Cr steel substrate, that was prefired at 400 °C and then Ni-YSZ anode layer was tape-casted, prefired at 600 °C and sprayed with an electrolyte. After that, cells were co-sintered at 1350 °C in H_2. The resulting YSZ electrolyte had a thickness of about 20 μm. Such fuel cell provided power densities of about 100 mW cm^{-2} at 800 °C and 200 mW cm^{-2} at 900 °C. Cells exhibited very good resistance to cyclic oxidation.

A mixed steel–ceramic porous composite is a subject of work reported by Matus et al. [17]. In this case the alumina titanate ceramic powders were mixed with 70Fe30Cr steel powders to lower thermal expansion coefficient. On top of this composite the YSZ electrolyte was deposited by tape casting, vacuum infiltration or colloidal spray formation. This multilayer SOFC was co-fired at 1350 °C for 4 h in reducing atmosphere. Best results were achieved for spray deposited cells. Thickness of sintered electrolyte was below 20 μm and the cells achieved maximum power density of about 350 mW cm^{-2} at 900 °C. High thermal conductivity of steel is also an advantage, because it allows rapid heat up of the cells. After 50 thermal cycles between 200 °C and 800 °C at heating and cooling rate of 50 °C min^{-1}, the cell has not shown degradation of power density.

Tucker et al. [18] prepared cell using porous stainless steel and achieved power densities of 285 mW cm^{-2} and 712 mW cm^{-2} at 700 °C in air and oxygen, respectively.

Currently, the most advanced design using porous metal-supported cells is a "TuffCell" constructed at Argonne National Laboratory. A self-contained complete SOFC buttons were prepared using 454 stainless steel and arranged to provide a stack [19]. Obtained power densities are on the level of 300 mW cm^{-2} at 800 °C.

Those works demonstrated the proof of principle for application of porous stainless steel as SOFC support. However, information about long-term properties of porous steels in SOFC working conditions is still not available.

2. Experimental

For preparation of porous substrates commercially available 430L stainless steel powder (∼mesh 100) from Hoeganaes, USA, was used. Index L means low carbon type 430 stainless steel. Samples were uni-axially compacted to obtain highly porous substrates. For all samples pressure of 100 MPa was used, which results in sample porosity above 40%. The porosity of samples was evaluated by the Archimedes method using kerosene as medium. Additives, lubricants or pore formers have not been added for sample formation. Temperatures of sintering were evaluated in order to ensure proper mechanical strength and electrical parameters. Sintering took place in a tube furnace with the flow of 100% H_2 at ∼100 sccm. Temperatures ranged from 800 °C to 1200 °C and dwell times from 1 h to 4 h. Philips-FEI XL30 ESEM scanning electron microscope was used to examine surface and cross-sections of samples after sintering. In some cases the 3% H_2O was added to H_2 by bubbling hydrogen through water bubbler at room temperature.

Cyclic thermogravimetry was performed at 400 °C and 800 °C in air and in 3%H_2O–97%H_2. These temperatures are chosen because they are regarded as lower and upper limits of intermediate temperature SOFCs operation. Moreover, the temperature of 800 °C is most widely used for evaluation of dense stainless steels [13]. Therefore it allows comparison between dense and porous properties of 430L stainless steel. The performance of porous metal-supported SOFCs was evaluated even at higher temperatures (e.g. 900 °C [16,17]), however probably

the temperature of 800 °C is a limit for their long-term operation [19]. The total time of thermogravimetric measurements is below 350 h. Mass gain of samples during this time is relatively high, so further characterization was neglected.

Mass change was calculated by comparing mass after designated oxidation time with initial mass

$$\left(\frac{\Delta m}{m}\right)_t = \frac{m_{t>0} - m_{t=0}}{m_{t=0}} \times 100\%, \quad (1)$$

where $m_{t=0}$ is the initial mass and $m_{t>0}$ is the mass after "t" hours of oxidation.

Weight measurement resolution was of 0.1 mg. Only time at soak temperature is taken into account. For oxidation in air and in humidified hydrogen samples were sintered at 1000 °C for 4 h. Porosity of those samples is approximately 45%. Additionally, the oxidation process was evaluated in humidified hydrogen at 800 °C for samples sintered at 800 °C and 1000 °C.

The electrical conductivity of steel was investigated on a series of steel samples sintered in dry hydrogen for 2 h. It was measured by Keithley 2400 SourceMeter using van der Pauw method (Fig. 1a).

Silver paste was used as contacts. Porosity of the samples is not taken into calculations. The porosities of those samples were about 45–55%. Conductivity versus temperature dependence after different oxidation times in 800 °C was measured for sample sintered in 800 °C.

Electrical resistance of oxide scale was evaluated using standard 4 probe technique (Fig. 1b). Sample was pre-oxidized for 40 h at 800 °C before painting the electrodes. Electrodes were prepared on opposite facets of the sample, each size of 1 cm × 1 cm using platinum paste (ESL 5542), which after deposition was sintered at 750 °C for 30 min. Current density was set to 300 mA cm^{-2} and voltage drop was measured using Hameg HM8112-2.

XRD spectra were collected by Philips X'Pert diffractometer after different times of oxidation in air and humidified hydrogen. Measurements were taken in air at room temperature using Cu Kα radiation. In all cases surface of the samples was studied. Qualitative analysis of diffraction spectra was carried out with ICDD PDF database [20]. In order to resolve similar spectra of isostructural iron oxide and chromium oxide Rietveld refinement analysis was performed [21].

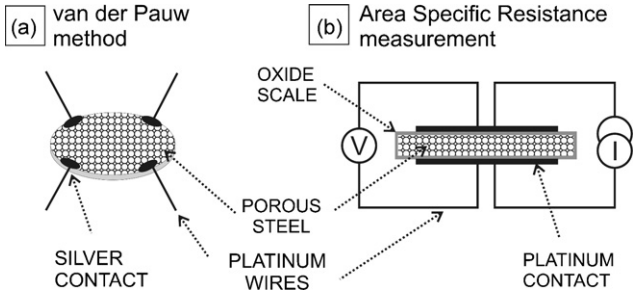

Fig. 1. Schematic diagrams of electrical conductivity measurements of conductivity of steel (a) and area-specific resistance (b).

3. Results

Sintering of steel powders in order to obtain porous substrates should take place above 900 °C. Below this temperature grains are not connected and sample is mechanically not rigid (Fig. 2b). Temperatures above 900 °C ensure good grain necking (Fig. 2a) and samples possess good mechanical properties. At temperatures of 1100 °C and above shrinkage of samples is observed. In all cases porosities were above 40% which ensures good gas permeability. Based on SEM images the evaluated surface roughness is approximately 20 μm, while the average pore diameters are also in the range of 20 μm. Such surface roughness and pore diameter can provide problems during deposition of thin layers. Ceramic anode substrates used for electrolyte supports usually have grain sizes in the range of few μm. As a result the pore sizes are greatly reduced in comparison to reported here. Smaller grains (higher mesh parameter) of steel would lower the pore sizes and minimize those problems. However, during the sintering step samples would loose their porosity. Usually smaller grain sizes promote higher densification, which is undesirable for SOFC support application. Microstructure of the inner part of the sample is similar to its surface. It is interesting to note, that in the SEM images of polished cross-section (Fig. 2c) the porosity seems to be smaller than that measured by Archimedes method.

Cyclic thermogravimetry measurements at 400 °C presented in Fig. 3 showed mass gain during oxidation in air, while in humidified hydrogen virtually no mass gain was observed. Mass gain is related to oxide scale formation on the steel surface. The weight gain as a function of time follows a parabolic rate law (Fig. 3). This type of mass gain can be related to a modified Wagner rate law. In its original form [22] the oxide thickness (or weight gain per unit area) versus time of oxidation is measured, which describes the oxide scale formation connected to the limiting process of an outward diffusion of the metal cations from bulk of the steel through scale to the surface. In this study it was necessary to modify the model due to evaluation of porous samples. Therefore, the relative mass change (from Eq. (1)) is measured as a function of time

$$\left(\frac{\Delta m}{m}\right)^2 = k_p t[\%^2], \quad (2)$$

where k_p is the parabolic rate constant and t is the time.

The results of thermogravimetry performed at 800 °C presented in Fig. 4 show oxide formation in both atmospheres, although oxides created are different, as will be described later. Oxidation in air is more rapid than in humidified hydrogen. Oxidation processes in both cases obey modified Wagner law.

Sintering temperature has visible influence on oxidation rate. As shown in Fig. 5, oxidation in humidified hydrogen of a sample sintered at 800 °C for 4 h is faster than that at 1000 °C. Porosities of the samples are the same within margin of 2%. The grains of samples sintered at 1000 °C are well bonded to each other (Fig. 2a). On the other hand the sintering temperature of 800 °C does not provide good contacts between grains (Fig. 2b).

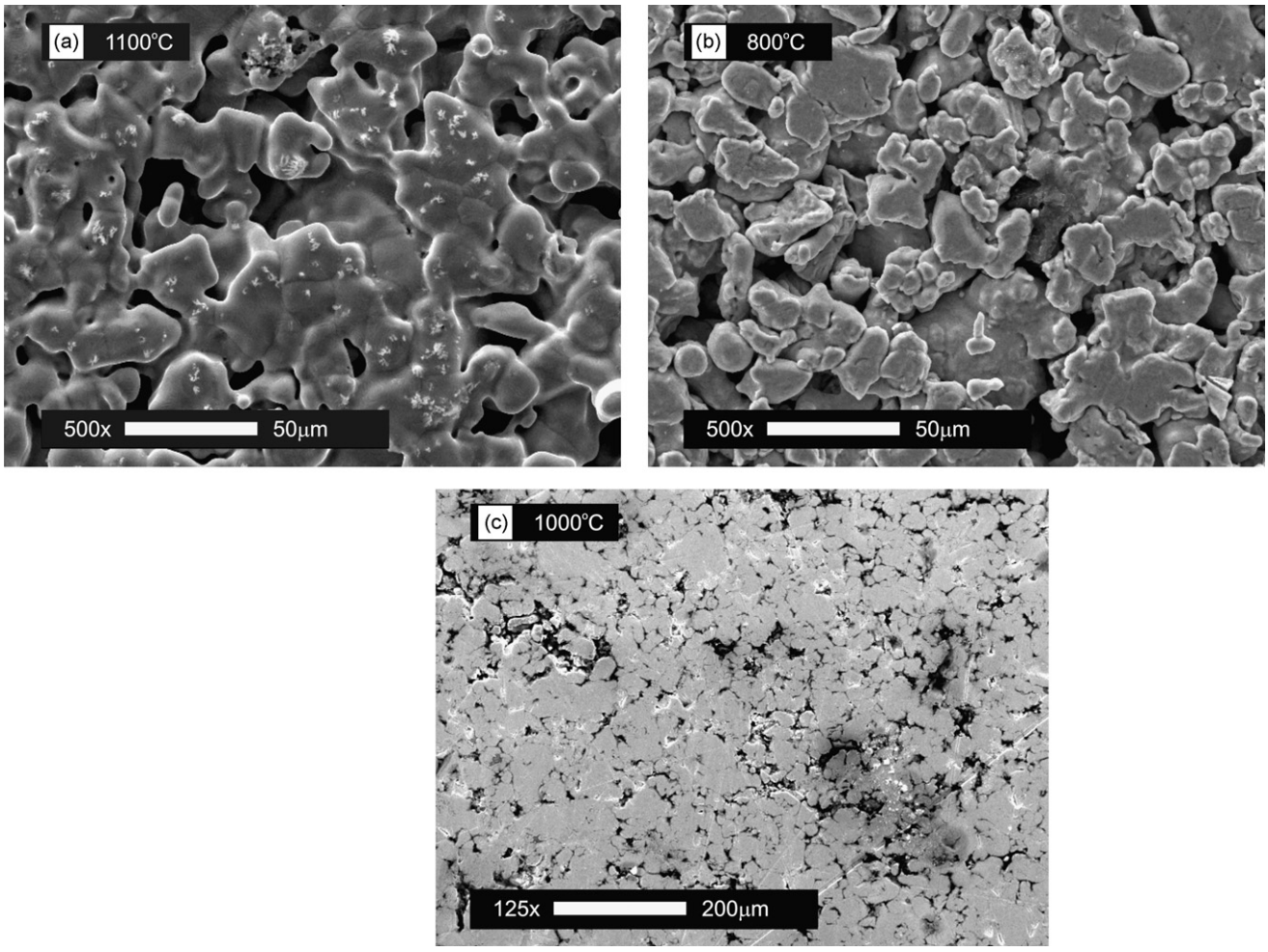

Fig. 2. SEM images of 430L surface sintered at 1100 °C (a) and at 800 °C (b) and cross-section of polished 430L sintered at 1000 °C (c).

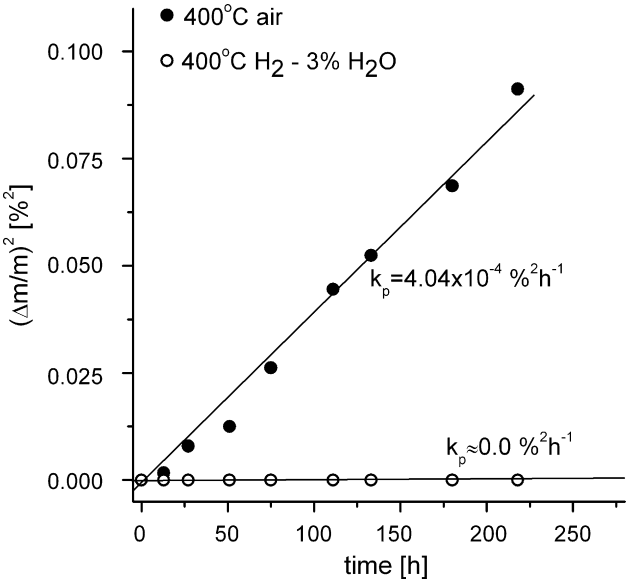

Fig. 3. Mass gain as a function of time for oxidation in air and in humidified hydrogen at 400 °C. Samples sintered at 1000 °C.

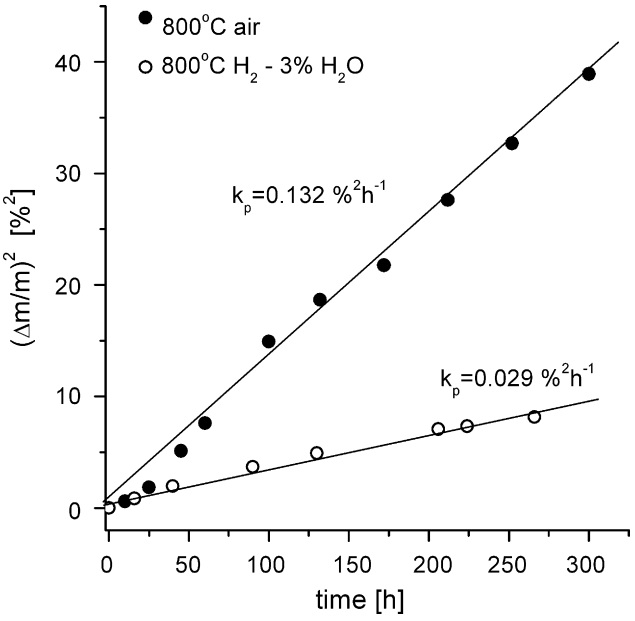

Fig. 4. Mass gain as a function of time for oxidation in air and in humidified hydrogen at 800 °C. Samples sintered at 1000 °C.

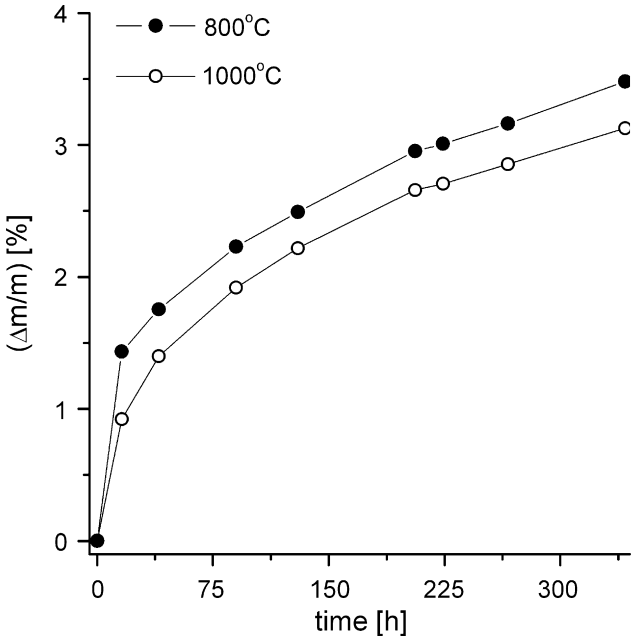

Fig. 5. Mass gain in humidified hydrogen at 800 °C as a function of time for samples sintered at 800 °C and 1000 °C.

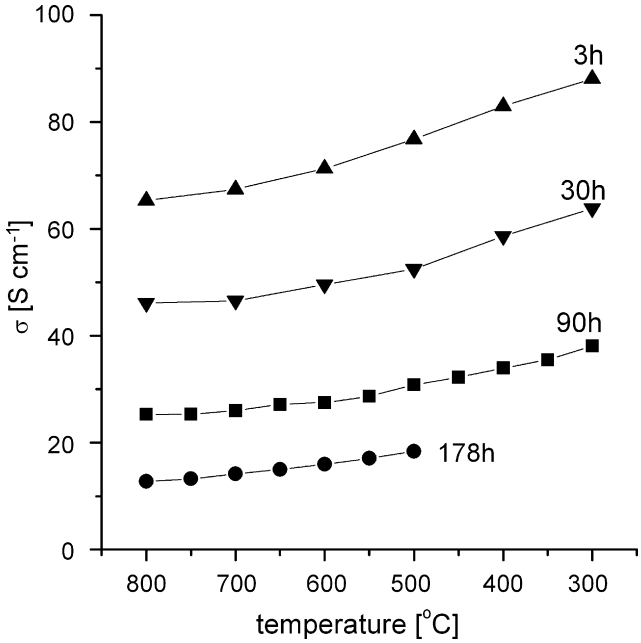

Fig. 7. 430L conductivity as a function of temperature after different times of oxidation in air at 800 °C.

Electrical conductivity of steel is strongly related to grain connections and thus is related to sintering temperature (Fig. 6). Samples prepared below 900 °C reveal relatively low electrical conductivity while sintered at 900 °C and above show metallic level of conductivity. In all cases electrical conductivity versus temperature shows metallic type conductivity. For comparison conductivity of steel sample without sintering step is shown. Conductivity versus oxidation time at 800 °C is shown in Fig. 7. Decrease of conductivity is clearly seen and after about 180 h the level of conductivity is almost one order of magnitude lower than at the beginning.

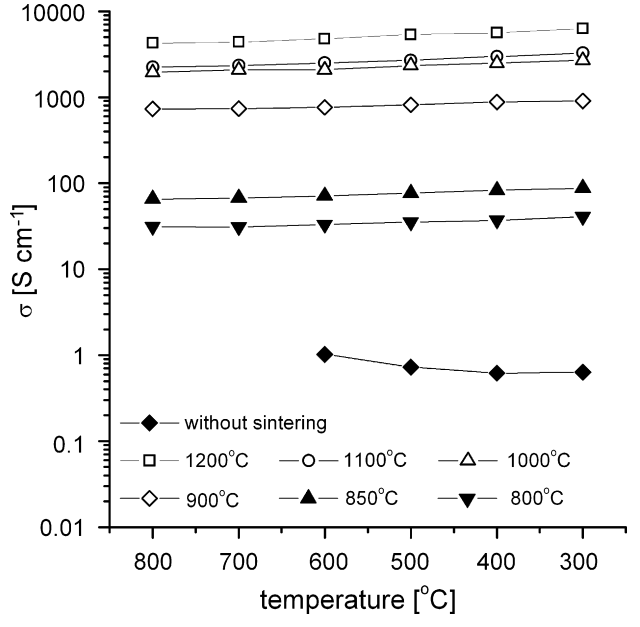

Fig. 6. Temperature dependence of 430L conductivity for different sintering temperatures.

Electrical conductivity of oxide scale measured at 800 °C in air is shown in Fig. 8. After about 30 h of measurement and total of about 75 h of soaking time at 800 °C, the area-specific resistance of oxide scale reaches level of 100 mΩ cm^2, which is considered as maximum allowable level for SOFC component [23]. This is unacceptable deterioration of stainless steel in comparison to expected operation time of fuel cell of about 40,000 h. The results obtained by Deng et al. [14] on dense 430 stainless steel show that the area-specific resistance reached 100 mΩ cm^2 after 500 h at 800 °C and after this time exhibited runaway increase of ASR. The rate of ASR change calculated from linear part of the plot in Fig. 8 is of about 3.3 mΩ cm^2 h^{-1}.

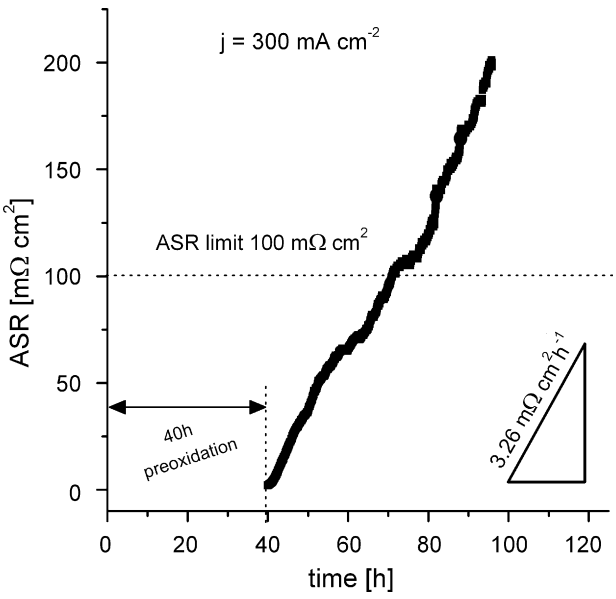

Fig. 8. Area-specific resistance of oxide scale formed on 430L in air at 800 °C.

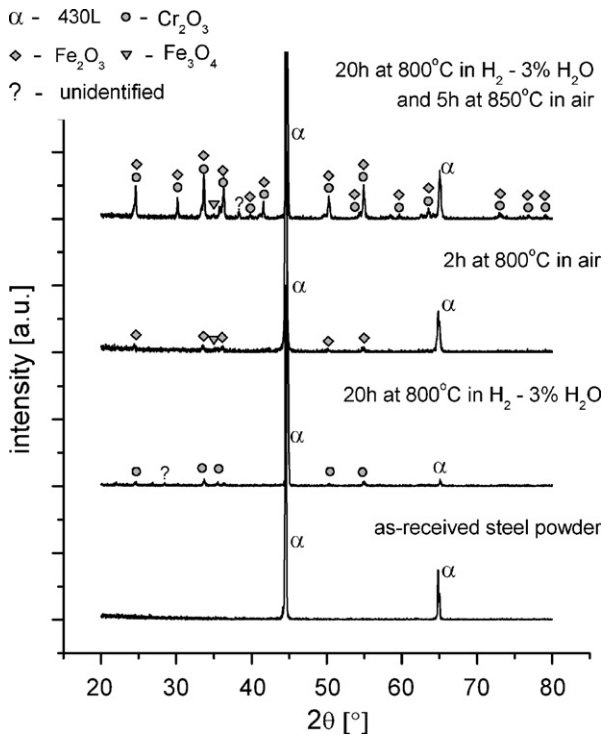

Fig. 9. XRD spectra before and after oxidation in air and humidified hydrogen. Due to isostructural nature of Fe_2O_3 and Cr_2O_3 Rietveld refinement method was used to distinguish the type of formed oxides.

The reported high level of contact resistance can be related to undesired iron oxide scale formation. Thus porous 430L is not regarded as a prospective for high-temperature fuel cells applications. In consequence porous 430L must be operated at lower temperature or coated with protective film in order to decrease area-specific resistance.

In Fig. 9 the XRD spectra of 430L oxidized in air and humidified hydrogen are presented. Spectra of as-received steel powder are also shown for comparison. Due to isostructural nature of Fe_2O_3 and Cr_2O_3 Rietveld refinement method was used to distinguish the type of formed oxides. In air the spectra shows that the oxide scale is composed mainly of Fe_2O_3. Some signs of $(Fe,Cr)_2O_3$ and Fe_3O_4 crystalline phases can also be observed. In humidified hydrogen mostly Cr_2O_3 scale is formed on the steel surface. This is also indicated by steel color. Samples oxidized in air are black in color while they are green when oxidized in humidified hydrogen. This corresponds to colors of dominating oxides phases. Formation of iron oxide in air is in contradiction with the results obtained for dense 430L [24]. In this case only the chromium oxide is formed both in air and in hydrogen. Different behavior of porous steel can be related to high specific surface area, which is available for oxidation. The chromium reservoir in bulk of the steel is probably insufficient to provide enough chromium for oxidation processes. Therefore other oxides, e.g. iron oxide can also be created. In case of the dense steel the chromium content of about 16–18% by weight ensures forming continuous protective chromium oxide [12–24].

4. Conclusions

The 430L stainless steel in dense form is regarded as possible candidate for SOFC interconnector. However, in recent years the idea has become very attractive to use porous stainless steel as a SOFC support. In this study the 430L stainless steel with desired porosity and mechanical properties was successfully prepared and evaluated. It can be noted that sintering above 900 °C is required to meet the demand for porous support. The oxidation of porous 430L is relatively fast due to its high specific surface area. The mass gain follows modified Wagner's law. Thermogravimetric measurements showed relatively high mass gain in air and in humidified hydrogen. It is related to formed oxide scale, which is composed mainly of Fe_2O_3 during oxidation in air. This scale is not regarded as prospective for SOFC operational conditions. The chromium content of about 16–18% is not enough to form protective chromium oxide scale. The Fe_2O_3 oxide scale also contributes to high area-specific resistance that after only 75 h of oxidation exceeded the level of 100 mΩ cm^2.

Acknowledgement

This work is supported by the project MNiSW 3 T10B 077 29.

References

[1] J. Will, A. Mitterdorfer, C. Kleinlogel, D. Perednis, L.J. Gauckler, Solid State Ionics 131 (2000) 79–96.
[2] M. Dokiya, Solid State Ionics 152/153 (2002) 383–392.
[3] B.C. Church, T.H. Sanders, R.F. Speyer, J.K. Cochran, Mater. Sci. Eng. A452/453 (2007) 334–340.
[4] Z. Yang, M.S. Walker, P. Singh, J.W. Stevenson, T. Norby, J. Electrochem. Soc. 151 (12) (2004) B669–B678.
[5] Z. Yang, G. Xia, G.D. Maupin, J.W. Stevenson, Surf. Coat. Technol. 201 (2006) 4476–4483.
[6] S.C. Paulson, V.I. Birss, J. Electrochem. Soc. 151 (11) (2004) A1961–A1968.
[7] Z. Yang, K.S. Weil, D.M. Paxton, J.W. Stevenson, J. Electrochem. Soc. 150 (9) (2003) A1188–A1201.
[8] J.E. Hammer, S.J. Laney, R.W. Jackson, K. Coyne, F.S. Pettit, G.H. Meier, Oxid. Met. 67 (2007) 1–38.
[9] J.W. Fergus, Mater. Sci. Eng. A397 (2005) 271–283.
[10] J. van Herle, R. Ihringer, R. Vasquez Cavieres, L. Constantin, O. Bucheli, J. Eur. Ceram. Soc. 21 (2001) 1855–1859.
[11] W.Z. Zhu, S.C. Deevi, Mater. Sci. Eng. A362 (2003) 228–239.
[12] T. Brylewski, T. Maruyama, M. Nanko, K. Przybylski, J. Therm. Anal. Calorim. 55 (1999) 681–690.
[13] T. Brylewski, M. Nanko, T. Maruyama, K. Przybylski, Solid State Ionics 143 (2001) 131–150.
[14] X. Deng, P. Wei, M.R. Bateni, A. Petric, J. Power Sources 160 (2006) 1225–1229.
[15] J. Carter, J. Ralph, J. Bae, T. Cruse, C. Rossignol, M. Krumpelt, R. Kumar, Fuel Cell 2002 Abstracts, Palm Springs, CA, 2002.
[16] I. Villarreal, C. Jacobson, A. Leming, Y. Matus, S. Visco, L. De Jonghe, Electrochem. Solid-State Lett. 6 (2003) A178–A179.
[17] Y.B. Matus, L. De Jonghe, C.P. Jacobson, S.J. Visco, Solid State Ionics 176 (2005) 443–449.
[18] M.C. Tucker, G.Y. Lau, C.P. Jacobson, L.C. DeJonghe, S.J. Visco, ECS Trans. 7 (2007) 279–286.
[19] J.D. Carter, J.-M. Bae, T.A. Cruse, J.M. Ralph, D.J. Myers, US Patent Application 0251947 A1 (2006).
[20] ICDD PDF-2 Database Release 1998, ISSN 1084-3116.

[21] The X'PERT PLUS Rietveld algorithm is based on the source codes of the program LHPM1 of R.J. Hill and C.J. Howard, X'Pert Plus, © 1999 Philips Electronics N.V, April 11, 1988.
[22] A. Atkinson, Rev. Mod. Phys. 57 (1985) 437–470.
[23] W.Z. Zhu, S.C. Deevi, Mater. Res. Bull. 38 (2003) 957–972.
[24] S.K. Yen, Y.C. Tsai, J. Electrochem. Soc. 143 (1996) 2493–2497.
[25] Stainless Steel Type 430 Technical Data Blue Sheet, ATI Allegheny Ludlum, 2007.
[26] Material Data Sheet No. 4046, ThyssenKrupp VDM, 2006.
[27] Stainless Steel E-brite Technical Data Blue Sheet, ATI Allegheny Ludlum, 2007.
[28] Haynes 230 Datasheet, Haynes International, 2004.